# Redox Behaviour of Pyrazolyl-Substituted 1,4-Dihydroxyarenes: Formation of the Corresponding Semiquinones, Quinhydrones and Quinones

Hans-Wolfram Lerner[a], Günter Margraf[a], Tonia Kretz[a], Olav Schiemann[b], Jan W. Bats[c], Gerd Dürner[c], Fabrizia Fabrizi de Biani[d], Piero Zanello[d], Michael Bolte[a], and Matthias Wagner[a]

[a] Institut für Anorganische Chemie, Johann Wolfgang Goethe-Universität Frankfurt am Main, Marie-Curie-Straße 11, D-60439 Frankfurt am Main, Germany
[b] Institut für Physikalische Chemie, Johann Wolfgang Goethe-Universität Frankfurt am Main, Marie-Curie-Straße 11, D-60439 Frankfurt am Main, Germany
[c] Institut für Organische Chemie, Johann Wolfgang Goethe-Universität Frankfurt am Main, Marie-Curie-Straße 11, D-60439 Frankfurt am Main, Germany
[d] Dipartimento di Chimica dell'Universita, Via Aldo Moro, I-53100 Siena, Italy

Reprint requests to Dr. Hans-Wolfram Lerner. E-mail: lerner@chemie.uni-frankfurt.de

Z. Naturforsch. **61b,** 252 – 264 (2006); received November 25, 2005

Pyrazolyl-substituted 1,4-dihydroxybenzene and 1,4-dihydroxynaphthene derivatives have been synthesized by reaction of 1,4-benzoquinone and 1,4-naphthoquinone, respectively, with pyrazole. Cyclovoltammetric measurements have shown that 1,4-benzoquinone possesses the potential to oxidize 2-(pyrazol-1-yl)- and 2,5-bis(pyrazol-1-yl)-1,4-dihydroxybenzene. The 2,5-bis(pyrazol-1-yl)-1,4-dihydroxybenzene reacts with air to give quantitatively black insoluble 2,5-bis(pyrazol-1-yl)-1,4-quinhydrone. Black crystals of 2,5-bis(pyrazol-1-yl)-1,4-quinhydrone suitable for X-ray diffraction were grown from methanol at ambient temperature (monoclinic $C2/c$). The poor yields of pyrazolyl-substituted 1,4-dihydroxybenzene and 1,4-dihydroxynaphthene derivatives can be explained by the formation of insoluble black quinhydrons in the reaction of benzoquinone and naphthoquinone with pyrazole. The dianions of 2-(pyrazol-1-yl)- and 2,5-bis(pyrazol-1-yl)-1,4-dihydroxybenzene react with oxygen to give the corresponding semiquinone anions. 2,5-Bis(pyrazol-1-yl)-1,4-benzoquinone shows two reversible one-electron reduction processes in cyclovoltammetric measurements, whereas pyrazolyl-substituted 1,4-dihdroxybenzene and -naphthene derivatives undergo irreversibile electron-transfer processes.

*Key words:* Quinhydrone, Semiquinone, Hydroquinone, Redoxactive Ligands, Crystal Structure

## Introduction

Redox-active ligands can be used to influence the electrochemical reactivity of transition metals since their redox activity is expanded upon complexation. The resulting complexes can undergo multi-electron transfer reactions which are the sum of the oxidation state changes of the metal center and the ligand [1, 2].

Due to their electrochemical reversibility, quinone derivatives are candidates for redox-active ligands. Oxidation of hydroquinone and reduction of benzoquinone derivatives are known to play an important role in biological redox processes [3]. The oxidation of the dianion of hydroquinone $\mathbf{1}^{2-}$ to benzoquinone **1ox** occurs in two one-electron steps *via* the semiquinone radical anion $\mathbf{1sq}^{-}$ (Scheme 1). However, this process depends strongly on the pH value.

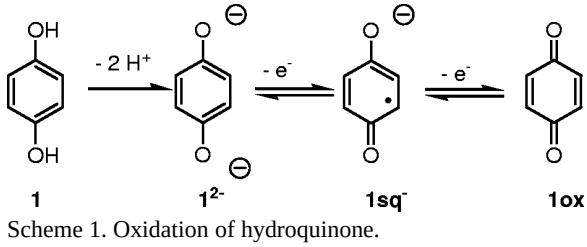


Scheme 1. Oxidation of hydroquinone.

Owing to their rigid structure and completely conjugated $\pi$-system, hydroquinone ligands can be expected to contribute efficiently to the spin-spin couplings between paramagnetic metal ions. In addition, the two diamagnetic compounds hydroquinone and benzoquinone as well as the paramagnetic semiquinone anion are able to interact with the orbitals of transition metals to different extents.

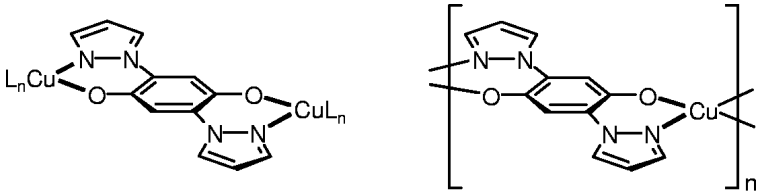


**A** **B**

Fig. 1. Dinuclear complex **A** and coordination polymer **B**.

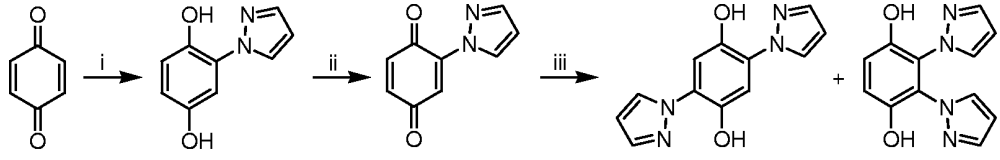


**2** **2ox** **3** **4**

Scheme 2. Formation of compounds **2**, **3**, and **4**. i = iii: 1,4-addition of pyrazole; ii = oxidation with 1,4-benzoquinone, elimination of hydroquinone.

By adding additional coordination sites, *para*-quinones can be derivatized to generate bidentate ligands. Promising members of this family of compounds are the derivatives of (pyrazol-1-yl)-1,4- dihydroxybenzene [4 – 7]. Therefore, we investigated the coordination behaviour of hydroquinone derivatives with chelating pyrazolyl anchor groups towards $Cu^{II}$ ions. We have established 2,5-bis(pyrazol-1-yl)-1,4-dihydroxybenzene as a redox-active bridging unit in dinuclear and polynuclear $Cu^{II}$ complexes **A** and **B** (Fig. 1) [8 – 13].

However, when 2-(pyrazol-1-yl)-1,4-dihydroxynaphthalene is reacted with $CuCl_2$ and lithium bis(trimethylsilyl)amide, no formation of $Cu^{II}$ complexes is observed. Instead, a redox reaction takes place in which $[Cu^{I}(NH_3)Cl]$ and 2-(pyrazol-1-yl)-1,4-naphtoquinone are formed [14]. It may thus be concluded that 2-(pyrazol-1-yl)-1,4-dihydroxynaphthalene not only acts as a proton source in the protolysis of lithium bis(trimethylsilyl)amide, but is also involved in the reduction of the $Cu^{II}$ centers. The purpose of the following paper is to investigate the electrochemical behaviour and the solid-state structures of several (pyrazol-1-yl)-1,4-dihydroxybenzene and (pyrazol-1-yl)-1,4-dihydroxynaphthalene derivatives. Finally we report on the crystal structure and the properties of 2,5-(bispyrazol-1-yl)-1,4-quinhydrone.

## Results and Discussion

### *Syntheses*

The reactions of 1,4-benzoquinone and 1,4-naphthoquinone with derivatives of pyrazole and triazole were first described by Gauß [15]. As reported previously, pyrazole adds to 1,4-benzoquinone to give a mixture of mono-pyrazolyl adduct **2** and bis-pyrazolyl adducts **3** and **4** (Scheme 2). Ballesteros and coworkers found that the relative amount of products thereby depends strongly on the reaction time [16].

In contrast to the results of earlier studies, investigations of our group have shown that a reaction between benzoquinone and hydroquinone **3** takes place to give quinone **3ox** and a black insoluble material. The addition of benzoquinone to pyrazole also produces a black precipitate. However, the solution of this reaction contains the hydroquinones **1**, **2**, **3**, and **4**. These hydroquinones have been identified by analytical HPLC. The stoichiometry of the reactants benzoquinone and pyrazole does not play an important role in product ratio as the reaction time does. However, under all the applied reaction conditions the yields of the hydroquinones **2**, **3** and **4** were quite low, which can be explained with the formation of the insoluble black quinhydrone **3qh**. The X-ray powder diffraction studies of this insoluble material have shown exclusively the pattern of **3qh**. It is interesting to note that if this reaction is carried out under inert gas, the sum of the yields of pyrazolyl-substituted hydroquinones is higher than the yields if benzoquinone reacts with pyrazole in air. We were interested in the preparation of hydroquinone **3** in large quantities. We therefore have optimized the reaction conditions to produce **3** in higher yield. The best result was obtained when the reaction was carried out in an inert gas atmosphere (*e.g.* nitrogen) with a ratio of benzoquinone to pyrazole of 1 : 1 in hot dioxane

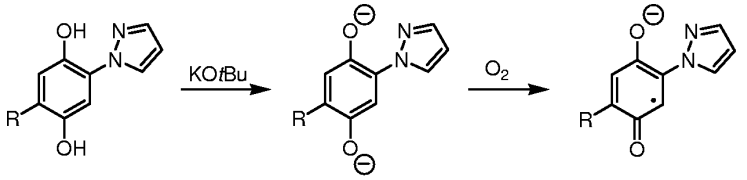


**2sq**$^-$ (R=H),
**3sq**$^-$ (R=pyrazol-1-yl)

Scheme 3. Synthesis of the semiquinone radical anions **2sq**$^-$ and **3sq**$^-$.

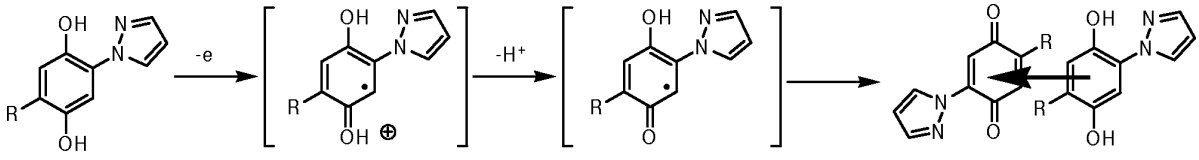


**2** (R=H),
**3** (R=pyrazol-1-yl)

**2sqH$_2^+$** (R=H),
**3sqH$_2^+$** (R=pyrazol-1-yl)

**2sq** (R=H),
**3sq** (R=pyrazol-1-yl)

**2qh** (R=H),
**3qh** (R=pyrazol-1-yl)

Scheme 4. Synthesis of the quinhydrone **2qh** and **3qh**.

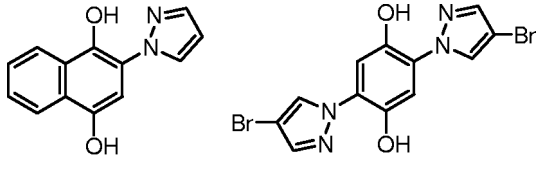

**5** **7**

Fig. 2. The hydroquinone derivatives **5** and **7**.

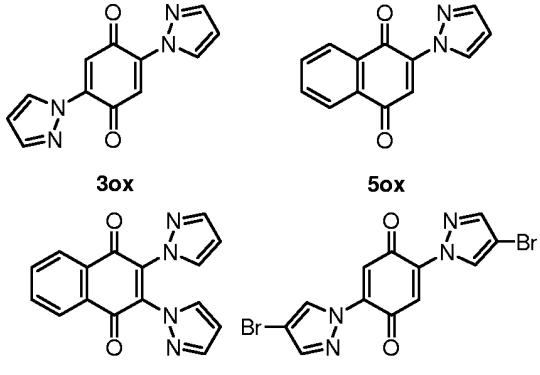

**3ox** **5ox**

**6ox** **7ox**

Fig. 3. The quinone derivatives **3ox**, **5ox**, **6ox** and **7ox**.

(yield 30%). The 1,4-hydroxybenzene derivatives **2**, **3**, and **4** have been separated by preparative HPLC and by crystallisation.

The 1,4-naphtohydroquinone **5** and the 1,4-hydroquinone **7** have been obtained following a similar synthesis protocol as described above for the preparation of **2**, **3**, and **4**. The syntheses of the quinone derivatives **3ox**, **5ox**, and **7ox** were conveniently achieved by oxidation of **3** with 1,4-benzoquinone and of **5** or **7** with 2,3-dichloro-5,6-dicyano-1,4-benzoquinone (DDQ). **6ox** has been prepared from 2,3-dichloro-1,4-naphthoquinone and pyrazole according to a literature procedure [15].

The hydroquinones **2**, **3**, **4**, and **5** can be deprotonated twice with 2 equivalents of a strong base such as KO*t*Bu. The resulting dianions show a pronounced sensitivity towards oxidation. The EPR spectra of isopropanol solutions of dianionic **2**$^{2-}$ and **3**$^{2-}$ in the presence of traces of oxygen show signals which can be assigned to the semiquinone anions **2sq**$^-$ and **3sq**$^-$ (Scheme 3).

Generally, semiquinone radical anions are only stable in solutions with a high pH value. In less alkaline solutions, a disproportionation reaction takes place from semiquinone to hydroquinone and quinone, as shown in Scheme 4. Equimolar mixtures of hydroquinone and benzoquinone are known to form intensively colored quinhydrones. These complexes show a charge transfer between the electron-rich hydroquinone and the electron-attracting benzoquinone (Scheme 4).

Upon standing in methanol under atmospheric conditions, the hydroquinone **3** is oxidized quantitatively to 2,5-bis(pyrazol-1-yl)-1,4-quinhydrone **3qh**. Black crystals of the quinhydrone **3qh** suitable for X-ray diffraction were obtained from methanol at ambient temperature. It is interesting to note that the quinhydrone **3qh** is nearly insoluble in organic solvents.

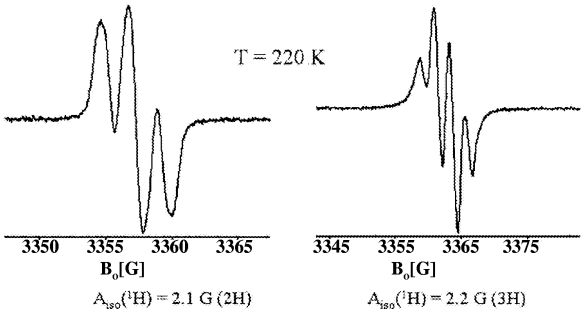


Fig. 4. Observed EPR spectra of the semiquinone anions **3sq**$^-$ (left) and **2sq**$^-$ (right).

*EPR spectra of the semiquinone anions 2sq*$^-$ *and 3sq*$^-$

Solid-state EPR spectroscopy has revealed the diamagnetic nature of 2,5-bis(pyrazol-1-yl)-1,4-quinhydrone **3qh**. The nature of this quinhydrone can also be observed in its IR spectrum, which is a superposition of the individual IR spectra of **3** and **3ox**. Similar IR patterns were observed for the parent compound **1qh** [17]. In the EPR spectrum of **2sq**$^-$ a four-line signal is observed, whereas **3sq**$^-$ shows a three-line signal (Fig. 4).

The multiplet splitting of the signals of the semiquinone anions **2sq**$^-$ and **3sq**$^-$ is caused by the coupling of an unpaired electron to protons attached to the central benzene ring {**2sq**$^-$: 3 H; (**3sq**$^-$): 2 H}. Couplings with pyrazolyl H substituents are not resolved for either semiquinone.

*Electrochemistry*

The electrochemical behaviour of **2**, **3**, **3ox**, and **5** has been investigated by cyclovoltammetry in dichloromethane solution. The cyclovoltammetric profiles exhibited by **2**, **3**, and **5** relate to oxidation processes; as expected, all of them possess features of chemical irreversibility on the cyclovoltammetric time scale (Scheme 4). The processes for **3** and **5** are all monoelectronic, whereas **2** shows a two-electron process. The unsubstituted parent hydroquinone undergoes a single two-electron oxidation at +1.25 V *vs.* S.C.E. in $CH_2Cl_2$.

Table 1. Formal electrode potentials (in V, vs SCE) for the oxidation processes of **2**, **3**, and **5** and for the reduction processes of **3ox** in dichloromethane solutions.

| | Oxidation | Reduction |
|---|---|---|
| **2** | +0.94*, +0.94* | |
| **3** | +0.90*, +1.10* | |
| **3ox** | | −0.29, −0.87 |
| **5** | +0.75*, +0.95* | |

* Irreversible process.

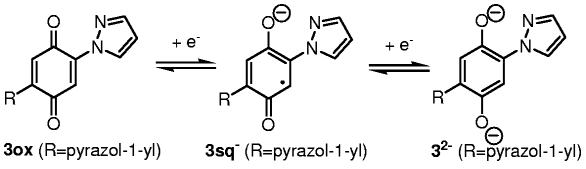


Scheme 5. Reduction of the quinone **3ox**.

In contrast to the hydroquinone derivatives **2**, **3**, and **5**, the quinone **3ox** shows two reversible one-electron reduction processes. The reduction of **3ox** can be explained with the formation of the semiquinone anion **3sq**$^-$ and the hydroquinone dianion $\mathbf{3}^{2-}$ as shown in Scheme 5.

*Structures*

The molecular structures of the compounds **3qh**, **4**, **5**, **5ox**, **6ox**, and **7ox** are shown in Figs 5 – 16. Selected bond lengths and angles are listed in the corresponding figure captions, details of the crystal structure analyses are summarized in Table 3.

The crystal structure determinations of **2**, **3**, **3ox**, and **4** · **(H$_2$O)** have already been reported [4, 18, 19]. We obtained single crystals suitable for X-ray diffraction of **2** from chloroform and carried out a redetermination of the structure at low temperature [20].

The quinhydrone **3qh** crystallizes in the monoclinic space group $C2/c$ with a crystallographically imposed

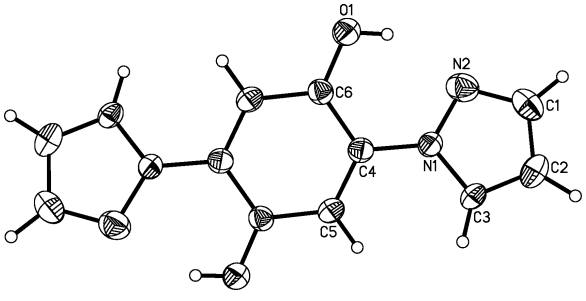


Fig. 5. Thermal ellipsoid plot of quinhydrone **3qh** showing the atom numbering scheme. The displacement ellipsoids are drawn at the 50% probability level. Selected bond lengths [Å] and torsion angles [°]: C(1)–C(2) 1.390(6), C(2)–C(3) 1.351(6), C(4)–C(5) 1.381(5), C(4)–C(6) 1.446(5), C(5)–C(6)#1 1.440(5), C(6)–O(1) 1.309(5), C(1)–N(2) 1.374(5), C(3)–N(1) 1.365(4), C(4)–N(1) 1.422(4), N(1)–N(2) 1.378(5), C(6)–C(4)–N(1)–N(2) −18.1(6). Hydrogen bonds [Å]: O(1)–H(10) 0.84, H(10)···N(2) 1.95, O(1)···N(2) 2.704(4), O(1)–H(10)···N(2) 149.2°. Symmetry transformations used to generate equivalent atoms: #1 $-x+1$, $-y+1$, $-z+1$.

Table 2. Selected bond lengths in [Å] in the solid state of **3** [4], **3qh** and **3ox** [18].

| | **3** | **3qh** | **3ox** |
|---|---|---|---|
| C(4)–C(5) | 1.383 | 1.381 | 1.335 |
| C(5)–C(6) | 1.383 | 1.440 | 1.467 |
| C(4)–C(6) | 1.396 | 1.446 | 1.508 |
| C(6)–O(1) | 1.361 | 1.309 | 1.221 |
| N(1)–C(4) | 1.425 | 1.422 | 1.409 |
| C(1)–N(2) | 1.332 | 1.365 | 1.324 |
| C(3)–N(1) | 1.364 | 1.365 | 1.362 |
| C(1)–C(2) | 1.382 | 1.390 | 1.399 |
| C(2)–C(3) | 1.361 | 1.351 | 1.364 |

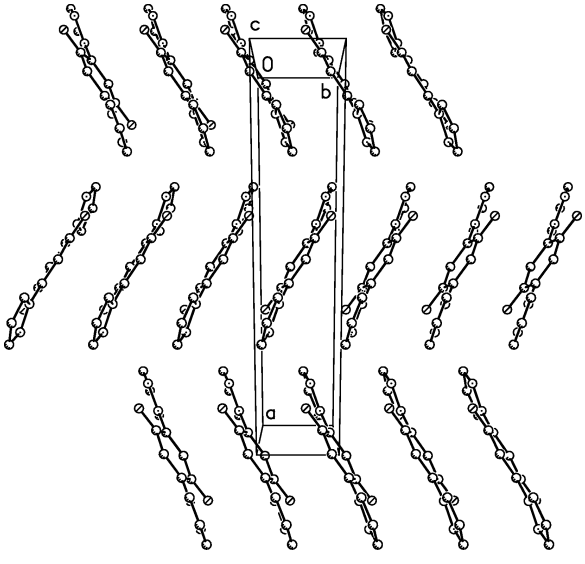


Fig. 6. Packing of the molecules of **3qh** in the unit cell.

inversion center at the midpoint of the benzene ring (Figs 5, 6, and 7). The C–C bond lengths of the central $C_6$-ring and the C-N and C–O distances at this ring are in between the values found in the structures of **3** and **3ox** (Table 2).

The pyrazolyl rings in **3qh** are slightly twisted off the hydroquinone plane with a torsion angle N(2)–N(1)–C(4)–C(6) of $-18.1(6)^\circ$. In the crystals of the quinhydrone **1qh**, the hydrogen bond formation leads to an infinite molecular chain along the molecular axis [21]. In the crystals of **3qh**, by contrast, the molecules form columns in which the benzoquinone rings are stacked with hydrogen bonds between the oxygen atoms of the two neighboring benzoquinone units (Fig. 6). In the solid-state structures of both quinhydrone **1qh** [21] and **3qh** intermolecular hydrogen bonds are established [**3qh**: O(1)–H(10) = 0.84 Å, H(10)···N(2) = 1.95 Å; O(1)–H(10)···N(2) = 149.2°], but the connectivity into infinite arrays is quite different. The molecular planes in **3qh** are shifted against each other in a stair-like manner. Remarkably, the IR spectrum of **3qh** as well as of **1qh** features the characteristic vibrations of the hydroquinones **3** and **1** and the quinones **3ox** and **1ox**, but the crystal structures of **3qh** and **1qh** show only one type of molecule. The distance in **3qh** between the molecular planes is about 3.2 Å and thus in a range typical for charge transfer complexes between two molecules.

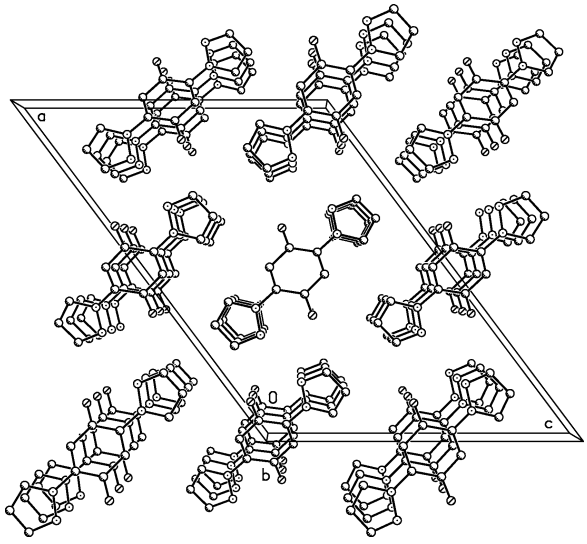


Fig. 7. Packing of the molecules of **3qh**. Projection along the *b*-axis.

The molecular structure of hydroquinone **4** (monoclinic space group $P2_1/c$ is shown in Fig. 8. Due to steric repulsion, the two pyrazole rings are twisted off the hydroquinone plane with torsion angles C(4)–C(3)–N(31)–N(32) of $-28.81(16)^\circ$ and C(1)–C(2)–N(21)–N(22) of $113.47(13)^\circ$. As shown in Fig. 9, the hydrogen bond network in the solid-state structure of **4** is quite different from that in **4** · **($H_2O$)**. One intramolecular hydrogen bond per molecule is established in **4** between O(4) and N(32) [O(4)–H(4) = 0.92(2) Å, H(4)···N(32) = 1.79(2) Å; O(4)–H(4)···N(32) = 148(2)°]. Furthermore, an intermolecular hydrogen bond occurs between O(1) and N(22)#1 [O(1)–H(1) = 0.88(2) Å, H(1)···N(22)#1 = 1.86(2) Å; O(1)–H(4)···N(22)#1 = 157.8(19)°].

2-(Pyrazol-1-yl)-1,4-dihydroxynaphthalene (**5**) crystallizes with two independent molecules in the asymmetric unit in the triclinic space group $P1$ (Fig. 10 represents one of two molecules of **5**; in the caption bond lengths and angles of both

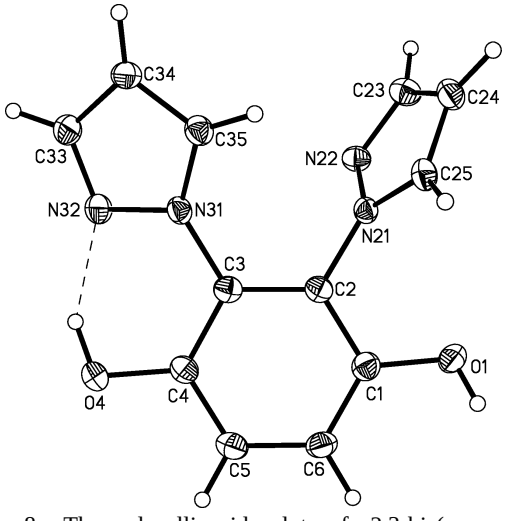


Fig. 8. Thermal ellipsoid plot of 2,3-bis(pyrazol-1-yl)-1,4-dihydroxybenzene **4**. The displacement ellipsoids are drawn at the 50% probability level. Selected bond lengths [Å] and torsion angles [°]: C(1)–C(2) 1.3980(17), C(2)–C(3) 1.4022(18), C(3)–C(4) 1.4053(18), C(4)–C(5) 1.3953(18), C(5)–C(6) 1.386(2), C(1)–O(1) 1.3547(16), C(4)–O(4) 1.3691(16), C(2)–N(21) 1.4231(16), N(21)–N(22) 1.3616(14), N(21)–C(25) 1.3562(17), N(22)–C(23) 1.3323(17), C(23)–C(24) 1.4018(18), C(24)–C(25) 1.3711(19), C(3)–N(31) 1.4275(15), N(31)–N(32) 1.3709(15), N(31)–C(35) 1.3607(16), N(32)–C(33) 1.3340(18), C(33)–C(34) 1.399(2), C(34)–C(35) 1.3745(18), C(1)–C(2)–N(21)–N(22) 113.47(13), C(4)–C(3)–N(31)–N(32) −28.81(16). Hydrogen bonds [Å]: O(1)–H(1) 0.88(2), H(1)···N(22)#1 1.86(2), O(1)···N(22)#1 2.6976(14), O(1)–H(1)···N(22)#1 157.8(19)°; O(4)–H(4) 0.92(2), H(4)···N(32) 1.79(2), O(4)···N(32) 2.6142(15), O(4)–H(4)···N(32) 148(2)°. Symmetry transformations used to generate equivalent atoms: #1 $x, -y+3/2, z+1/2$.

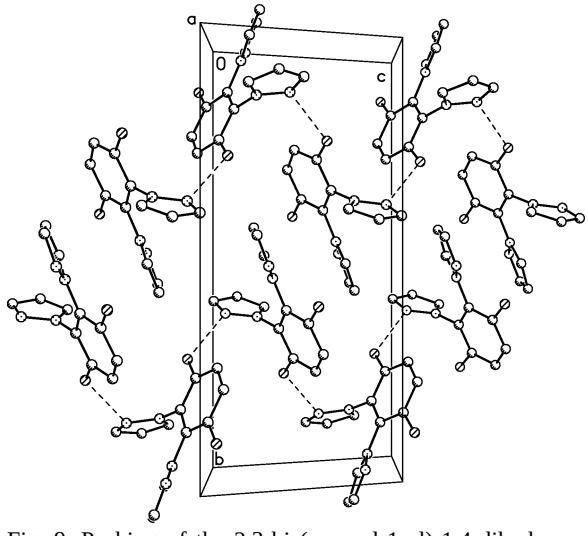


Fig. 9. Packing of the 2,3-bis(pyrazol-1-yl)-1,4-dihydroxybenzene molecules **4**.

molecules are listed). Intramolecular hydrogen bonds are established between O(2) and N(12) [O(2)–H(2) = 0.84 Å, H(2)···N(12) = 1.81 Å; O(2)–H(2)···N(12) = 146.6°]. Due to this hydrogen bond, the pyrazole and naphthoquinone planes in **5** are nearly coplanar with a torsion angle C(2)–C(1)–N(11)–N(12) of −4.5(9)°. In addition, intermolecular hydrogen bonds are found between O(9) and O(2A)#1 [O(9)–H(9) = 0.84 Å, H(9)···O(2A)#1 = 2.05 Å; O(9)–H(9)···O(2A)#1 = 168.1°].

2-(Pyrazol-1-yl)-1,4-naphtoquinone (**5ox**) was obtained in two different polymorphs, one in the monoclinic space group $C2/c$, Fig. 11, the other one in the orthorhombic space group $Pna2_1$, Fig. 12. The angle between the pyrazole plane and the naphthoquinone plane is 20.7° in the monoclinic polymorph of **5ox**. The structure of orthorhombic polymorph of **5ox** features two independent molecules (Fig. 12), which possess angles between the pyrazole plane and the naphthoquinone plane of 18.8° and 20.6°, respectively. In the quinone fragment of the orthorhombic polymorph of **5ox** the C(4)–C(5) and C(17)–C(18) bonds are about 0.04 Å shorter than the C(2)–C3 and C(15)–C(16) bonds. This may result from resonance in the segments O(2)–C(5)–C(4)–C(3)–N(1) and O(4)–C(18)–C(17)–C(16)–N(3). Each molecule shows two intramolecular contacts which approach the van der Waals contact distances [H(4)···N(2): 2.43 Å, H(13)···O(1): 2.40 Å, H(17)···N(4): 2.44 Å, H(26)···O(3): 2.36 Å]. As shown in Fig. 13, stacks of molecules are found in the crystallographic b-direction. Molecules within each stack are connected by a number of $\pi\cdots\pi$-contacts. The packing of the molecules also shows three intermolecular C–H···O interactions with H···O distances between 2.39 and 2.47 Å and C–H···O angles between 144 and 147°.

2,3-Bis(pyrazol-1-yl)-1,4-naphthoquinone (**6ox**) crystallizes in the orthorhombic space group *Pccn* (Fig. 14). Due to steric repulsion, the two pyrazole rings are twisted off the naphthoquinone plane with torsion angles C(1)–C(2)–N(21)–N(22) of −128.75(10)° and C(4)–C(3)–N(31)–N(32) of −141.32(10)°.

The molecular structure of **7ox** is shown in Fig. 15. The compound crystallizes in the monoclinic space group $C2/c$. The two Br-substituted pyrazole rings are

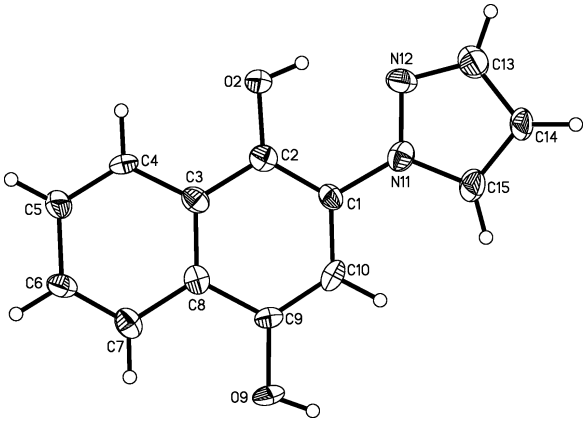


Fig. 10. Thermal ellipsoid plot of one from two independent molecules in the asymmetric unit of 2-(pyrazol-1-yl)-1,4-dihydroxynaphthalene **5**. The displacement ellipsoids are drawn at the 50% probability level. Selected bond lengths [Å] and torsion angles [°]: C(1)–C(2) 1.383(9), C(1)–C(10) 1.398(9), C(2)–C(3) 1.418(8), C(3)–C(4) 1.420(9), C(3)–C(8) 1.417(9), C(4)–C(5) 1.357(9), C(5)–C(6) 1.438(9), C(6)–C(7) 1.352(9), C(7)–C(8) 1.431(8), C(8)–C(9) 1.448(9), C(9)–C(10) 1.365(9), C(1)–N(11) 1.441(8), C(2)–O(2) 1.368(7), C(9)–O(9) 1.377(7), N(11)–N(12) 1.347(8), N(11)–C(15) 1.360(8), N(12)–C(13) 1.307(9), C(13)–C(14) 1.394(10), C(14)–C(15) 1.390(9), C(2)–C(1)–N(11)–N(12) −4.5(9). Hydrogen bonds [Å]: O(2)–H(2) 0.84, H(2)···N(12) 1.81, O(2)···N(12) 2.553(7), O(2)–H(2)···N(12) 146.6°; O(9)–H(9) 0.84, H(9)···O(2A)#1 2.05, O(9)···O(2A)#1 2.876(7), O(9)–H(9)···O(2A)#1 168.1°. Selected bond lengths [Å] and torsion angles [°] of the second molecule: C(1A)–C(2A) 1.391(9), C(1A)–C(10A) 1.393(9), C(1A)–N(11A) 1.436(8), C(2A)–C(3A) 1.453(9), C(3A)–C(4A) 1.430(9), C(3A)–C(8A) 1.396(10), C(4A)–C(5A) 1.362(10), C(5A)–C(6A) 1.392(10), C(6A)–C(7A) 1.347(10), C(7A)–C(8A) 1.431(10), C(8A)–C(9A) 1.453(9), C(9A)–C(10A) 1.376(9), C(1A)–N(11A) 1.436(8), C(2A)–O(2A) 1.339(8), C(9A)–O(9A) 1.376(8), N(11A)–N(12A) 1.342(8), N(11A)–C(15A) 1.365(8), N(12A)–C(13A) 1.338(9), C(13A)–C(14A) 1.373(10), C(14A)–C(15A) 1.372(10), C(2A)–C(1A)–N(11A)–N(12A) −1.4(8). Hydrogen bonds [Å]: O(2A)–H(2A) 0.84, H(2A)···N(12A) 1.83, O(2A)···N(12A) 2.568(7), O(2A)–H(2A)···N(12A) 145.0°; O(9A)–H(9A) 0.84, H(9A)···O(2)#2 1.96, O(9A)···O(2)#2 2.798(7), O(9A)–H(9A)···O(2)#2 171.9°. Symmetry transformations used to generate equivalent atoms: #2 $x+1$, $-y+1$, $-z+2$.

almost in a common plane as depicted in Fig. 16. A structural motif similar to that of the quinone **7ox** has also been found for the hydroquinone derivative **3** [4, 19]. However, the hydroquinone **3** displays intramolecular hydrogen bonds between the OH groups of the hydroquinone fragments and the

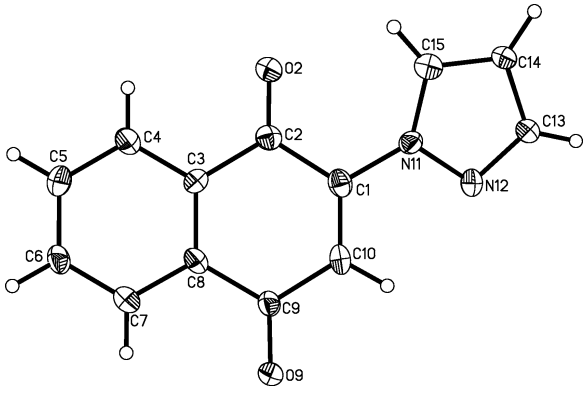


Fig. 11. Thermal ellipsoid plot of 2-(pyrazol-1-yl)-1,4-naphthoquinone **5ox** (monoclinic polymorph). The displacement ellipsoids are drawn at the 50% probability level. Selected bond lengths [Å] and torsion angles [°]: C(1)–C(2) 1.511(10), C(1)–C(10) 1.358(10), C(2)–C(3) 1.509(10), C(3)–C(4) 1.407(10), C(3)–C(8) 1.420(9), C(4)–C(5) 1.414(10), C(5)–C(6) 1.402(10), C(6)–C(7) 1.405(10), C(7)–C(8) 1.418(10), C(8)–C(9) 1.510(10), C(9)–C(10) 1.490(10), C(1)–N(11) 1.447(9), C(2)–O(2) 1.235(9), C(9)–O(9) 1.252(8), N(11)–N(12) 1.386(8), N(11)–C(15) 1.384(9), N(12)–C(13) 1.364(9), C(13)–C(14) 1.439(10), C(14)–C(15) 1.365(11), C(2)–C(1)–N(11)–N(12) –159.2(6).

pyrazolyl nitrogen atoms. As shown in Fig. 16 the quinone **7ox** forms a layer structure in the solid state. It is interesting to note that the molecular structure of **7ox** is quite different from that of **3ox**. In the quinone derivative **3ox** [18] the pyrazolyl rings are turned almost 180° about the axis.

## Conclusion

In summary, cyclovoltammetric measurements have shown that 1,4-benzoquinone possesses a higher oxidation potential than the pyrazolyl-substituted quinones **2ox**, **3ox**, and **5ox** and is therefore able to oxidize the pyrazolyl-substituted hydroquinones **2**, **3**, and **5**. Moreover, the hydroquinone **3** reacts with air to give the black insoluble quinhydrone **3qh** quantitatively. In the syntheses of the hydroquinone derivatives **2**, **3**, **4**, and **5** the corresponding quinhydrones are generated as side products. The formation of these insoluble black quinhydrone derivatives in the reaction of 1,4-benzoquinone or 1,4-naphtoquinone with pyrazole can explain the poor yields of **2**, **3**, **4**, and **5**. The syntheses of the quinone derivatives **3ox**, **5ox**, and **7ox** were conveniently achieved by oxidation of **3** with 1,4-benzoquinone and of **5** or **7** with 2,3-dichloro-5,6-dicyano-1,4-benzoquinone.

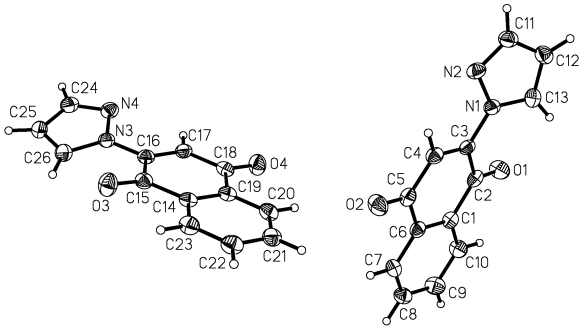


Fig. 12. Thermal ellipsoid plot of 2-(pyrazol-1-yl)-1,4-naphthoquinone **5ox** (orthorhombic polymorph). The displacement ellipsoids are drawn at the 50% probability level. Selected bond lengths [Å] and torsion angles [°]: C(1)–C(2) 1.490(3), C(1)–C(6) 1.399(3), C(1)–C(10) 1.388(3), C(2)–C(3) 1.492(3), C(3)–C(4) 1.345(3), C(4)–C(5) 1.454(3), C(5)–C(6) 1.483(3), C(6)–C(7) 1.391(3), C(7)–C(8) 1.383(3), C(8)–C(9) 1.387(3), C(9)–C(10) 1.389(3), C(3)–N(1) 1.408(3), C(2)–O(1) 1.229(3), C(5)–O(2) 1.227(2), N(1)–N(2) 1.372(2), N(1)–C(13) 1.374(3), N(2)–C(11) 1.321(3), C(12)–C(11) 1.406(3), C(12)–C(13) 1.361(3), C(14)–C(15) 1.493(3), C(14)–C(19) 1.388(3), C(14)–C(23) 1.397(3), C(14)–C(15) 1.493(3), C(15)–C(16) 1.505(3), C(16)–C(17) 1.339(3), C(17)–C(18) 1.464(3), C(18)–C(19) 1.484(3), C(19)–C(20) 1.398(3), C(20)–C(21) 1.384(3), C(21)–C(22) 1.385(3), C(22)–C(23) 1.384(3), C(16)–N(3) 1.410(3), C(15)–O(3) 1.216(3), C(18)–O(4) 1.234(3), N(3)–N(4) 1.374(2), N(3)–C(26) 1.367(3), N(4)–C(24) 1.325(3), C(24)–C(25) 1.398(3), C(25)–C(26) 1.361(3), N(2)–N(1)–C(3)–C(2) 161.28(18), N(4)–N(3)–C(16)–C(15) 162.02(19).

## Experimental Section

Reagents and solvents were obtained from Aldrich Chemicals. NMR spectra were run at ambient temperature. NMR: Bruker AMX 250, Bruker DPX 250, Bruker AMX 400 spectrometers. Abbreviations: s = singlet; d = doublet; tr = triplet; vtr = virtual triplet; nr = multiplet expected in the $^1$H NMR spectrum, but not resolved; pz = pyrazolyl; hqui = hydroquinone. Infrared spectra were taken of solid samples in KBr on a Nicolet Magna IR 550 spectrometer. ESI-MS: Fisons (now Micromass) VG Platform II. Elemental analyses (carried out at the Institut für Organische Chemie, Universität Frankfurt): Foss-Heraeus CHN-O-Rapid.

*Addition of pyrazole to benzoquinone*

The reaction protocol was performed under different conditions:

Method A: Reaction of one equivalent of 1,4-benzoquinone and two equivalents of pyrazole in air.

Method B: Reaction of one equivalent of 1,4-benzoquinone and one equivalent of pyrazole in air.

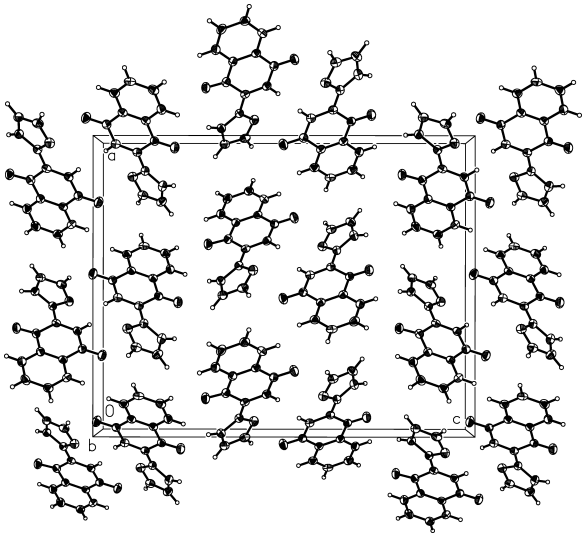


Fig. 13. Packing of the **5ox** molecules (orthorhombic polymorph) in the unit cell.

Method C: Reaction of one equivalent of 1,4-benzoquinone and one equivalent of pyrazole in a nitrogen atmosphere.

General protocol: 1,4-Benzoquinone and pyrazole were heated in dioxane under reflux for 1 h. The hot reaction mixtures were filtered and the filtrates were taken to dryness *in vacuo*.

The relative amounts of **1**–**4** in these reaction mixtures were determined by analytical HPLC (Merck $C_{18}$; Merck Hitachi L4000A UV detector, $\lambda = 254$ nm; flow rate: 0.8 ml min$^{-1}$) with gradient elution (0.1 M trifluoroacetic acid / methanol). 2 mg of each of the dried filtrates were redissolved in 2 ml 0.1 M trifluoroacetic acid / methanol and used for analysis.

*Preparation of* **2**, **3**, *and* **4**: Pyrazole (12.94 g, 190 mmol) and 1,4-benzoquinone (20.54 g, 190 mmol) were heated in dioxane for one hour in an atmosphere of nitrogen. The hot solution was filtered, the filtrate was taken to dryness *in vacuo*. The residue was dissolved in a minimum amount of $CHCl_3$. Addition of ethanol led to precipitation of **3**. The mother liquor was taken to dryness *in vacuo* and **2** and **4** were separated with preparative HPLC. Recrystallisation ($CHCl_3$) of the crude material afforded compound **3** (30%) as colorless needles.

For quantitative separations, the dried filtrate was redissolved and separated by HPLC (Nucleoprep, 650 mm × 50 mm, 20 $\mu$m, Macherey-Nagel, Germany; Merck Hitachi L4000A UV detector, $\lambda = 254$ nm; SepTech Refractive Index Monitor) with isocratic elution. A typical separation was performed with a flow rate of 0.1 l min$^{-1}$, using a three-solvent system (hexane/ethylacetate/dichloromethane 1 : 1 : 2).

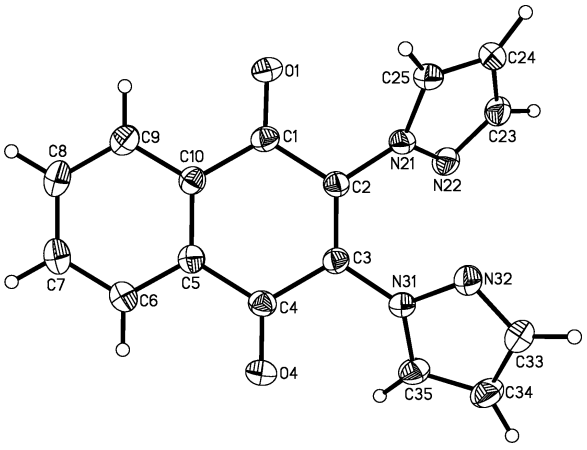


Fig. 14. Thermal ellipsoid plot of 2-(Pyrazol-1-yl)-1,4-naphthoquinone **6ox**. The displacement ellipsoids are drawn at the 50% probability level. Selected bond lengths [Å] and torsion angles [°]: C(1)–C(2) 1.4941(15), C(1)–C(10) 1.4838(15), C(2)–C(3) 1.3568(15), C(3)–C(4) 1.5062(15), C(4)–C(5) 1.4851(15), C(5)–C(6) 1.3963(15), C(5)–C(10) 1.3971(16), C(6)–C(7) 1.3876(17), C(7)–C(8) 1.3891(19), C(8)–C(9) 1.3896(17), C(9)–C(10) 1.3951(16), C(1)–O(1) 1.2208(14), C(4)–O(4) 1.2180(14), C(2)–N(21) 1.4105(14), N(21)–N(22) 1.3685(13), N(21)–C(25) 1.3610(14), N(22)–C(23) 1.3238(15), C(23)–C(24) 1.4057(19), C(24)–C(25) 1.3627(17), C(3)–N(31) 1.4005(14), N(31)–N(32) 1.3756(13), N(31)–C(35) 1.3735(15), N(32)–C(33) 1.3208(16), C(33)–C(34) 1.4069(19), C(34)–C(35) 1.3579(18), C(1)–C(2)–N(21)–N(22) −128.75(10); C(4)–C(3)–N(31)–N(32) −141.32(10).

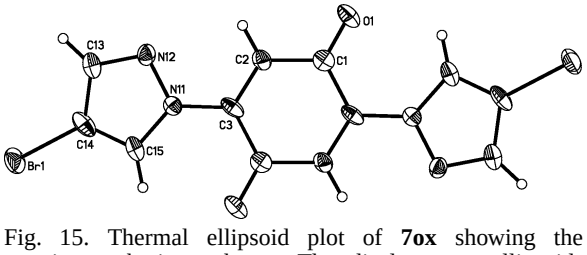


Fig. 15. Thermal ellipsoid plot of **7ox** showing the atomic numbering scheme. The displacement ellipsoids are drawn at the 50% probability level. Selected bond lengths [Å] and angles [°]: Br(1)-C(14) 1.893(8), O(1)-C(1) 1.233(11), C(1)-C(3)#1 1.482(14), C(1)-C(2) 1.489(12), C(2)-C(3) 1.343(11), C(3)-N(11) 1.431(11), C(3)-C(1)#1 1.482(14), N(11)-C(15) 1.374(12), N(11)-N(12) 1.378(10), N(12)-C(13) 1.338(13), C(13)-C(14) 1.427(15), C(14)-C(15) 1.360(14), O(1)-C(1)-C(3)#1 123.1(8), O(1)-C(1)-C(2) 119.0(9), C(3)#1-C(1)-C(2) 118.0(7), C(3)-C(2)-C(1) 121.4(9), C(2)-C(3)-N(11) 120.0(9), C(2)-C(3)-C(1)#1 120.5(8), N(11)-C(3)-C(1)#1 119.4(7), C(15)-N(11)-N(12) 111.6(7), C(15)-N(11)-C(3) 129.6(8), N(12)-N(11)-C(3) 118.8(7), C(13)-N(12)-N(11) 106.0(8), N(12)-C(13)-C(14) 108.8(10), C(15)-C(14)-C(13) 107.8(8), C(15)-C(14)-Br(1) 126.7(8), C(13)-C(14)-Br(1) 125.4(8), C(14)-C(15)-N(11) 105.7(9).

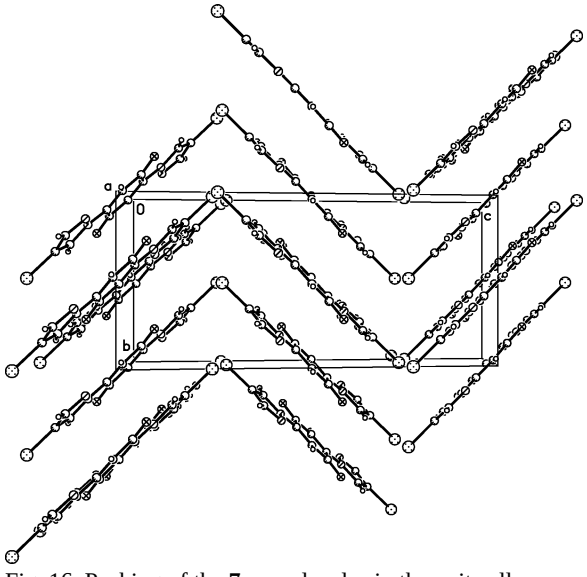


Fig. 16. Packing of the **7ox** molecules in the unit cell.

*2-(Pyrazol-1-yl)-1,4-dihydroxybenzene* (**2**): $^1$H NMR (250 MHz, $CDCl_3$): $\delta = 4.68$ (s, 1 H), 6.48 (dd, $J = 2.25$ Hz, 1 H), 6.64 (dd, $J = 8.75$ Hz, 1 H), 6.90 (d, $J = 2.5$ Hz, 1 H), 6.95 (d, $J = 3.75$ Hz, 1 H), 7.71 (d, $J = 1.25$ Hz, 1 H), 7.92 (d, $J = 2.0$ Hz, 1 H), 10.86 (s, 1 H). HPLC: $\tau = 14.57$ min. MS (ESI): $m/z = 176$ [$M^+$]. $C_9H_8N_2O_2$ (176.17): calcd. C 61.36, H 4.58, N 15.90; found C 61.61, H 4.48, N 15.62.

*2,5-Bis(pyrazol-1-yl)-1,4-dihydroxybenzene* (**3**): $^1$H NMR (250 MHz, $CDCl_3$): $\delta = 6.50$ (dd, $J = 2.0$ Hz, 2 H), 7.12 (s, 2 H), 7.72 (d, $J = 1.5$ Hz, 2 H), 7.95 (d, $J = 2.25$ Hz, 2 H), 11.13 (s, 2 H). IR (KBr): $\upsilon_{max} = 1542$, 1538, 1535 $cm^{-1}$. HPLC: $\tau = 10.86$ min. MS (ESI): $m/z = 242$ [$M^+$]. $C_{12}H_{10}N_4O_2$ (242.24): calcd. C 59.50, H 4.16, N 23.13; found C 59.74, H 4.13, N 22.96.

*2,3-Bis(pyrazol-1-yl)-1,4-dihydroxybenzene* (**4**): $^1$H NMR (250 MHz, $CDCl_3$): $\delta = 6.32$ (dd, 2 H, $J = 2.25$ Hz), 6.82 (d, 2 H, $J = 2.5$ Hz), 7.02 (s, 2 H), 7.79 (d, 2 H, $J = 2.0$ Hz), 8.31 (s, 2 H). HPLC: $\tau = 17.77$ min. MS (ESI): $m/z = 242$ [$M^+$]. $C_{12}H_{10}N_4O_2$ (242.24): calcd. C 59.50, H 4.16, N 23.13; found C 59.37, H 4.06, N 22.79.

### *Oxidation of* **3**

*Preparation of* **3ox**: A solution of 1,4-benzoquinone (0.110 g, 1 mmol) in 30 ml of dioxane was added dropwise to a stirred solution of 2,5-bis(pyrazol-1-yl)-1,4-dihydroxybenzene (0.242 g, 1 mmol) in 30 ml dioxane at r. t. After the mixture had been stirred for one hour, the orange mother liquor was filtered off the precipitate, taken to dryness *in vacuo*, redissolved in a minimum amount of dichloromethane, filtered, and taken to dryness again. Recrystallisation (dichloromethane) of this material afforded

Table 3. Crystallographic data and further details of the structure determination of **3qh**, **4**, **5**, **5ox**, **6ox**, and **7ox**.

| | **3qh** | **4** | **5** | **5ox** | **5ox** | **6ox** | **7ox** |
|---|---|---|---|---|---|---|---|
| Empirical formula | $C_{12}H_9N_4O_2$ | $C_{12}H_{10}N_4O_2$ | $C_{13}H_{10}N_2O_2$ | $C_{13}H_8N_2O_2$ | $C_{13}H_8N_2O_2$ | $C_{16}H_{10}N_4O_2$ | $C_{12}H_6Br_2N_4O_2$ |
| Color | black | colorless | colorless | yellow | brown | orange | orange |
| Formula weight | 241.23 | 242.24 | 226.23 | 224.21 | 224.21 | 290.28 | 398.03 |
| Crystal system | monoclinic | monoclinic | triclinic | monoclinic | orthorhombic | orthorhombic | monoclinic |
| Space group | $C2/c$ | $P2_1/c$ | $P\bar{1}$ | $C2/c$ | $Pna2_1$* | $Pccn$ | $C2/c$ |
| $a$, Å | 21.629(4) | 8.1195(7) | 9.438(2) | 16.432(6) | 17.876(6) | 12.3016(7) | 7.8358(9) |
| $b$, Å | 3.7334(9) | 17.7566(12) | 10.145(2) | 12.686(3) | 5.0233(13) | 28.861(2) | 8.5800(11) |
| $c$, Å | 16.045(3) | 8.7302(8) | 11.697(2) | 11.481(4) | 22.644(5) | 7.3643(5) | 19.1900(17) |
| $\alpha$, deg | 90 | 90 | 75.680(10) | 90° | 90° | 90° | 90 |
| $\beta$, deg | 126.850(10) | 116.352(7) | 78.430(10) | 121.32(3)° | 90° | 90° | 101.563(8) |
| $\gamma$, deg | 90 | 90 | 76.820(10) | 90° | 90° | 90° | 90 |
| Volume, (Å$^3$), $Z$ | 1036.8(4), 4 | 1127.88(16), 4 | 1044.2(4), 4 | 2044.5(11), 8 | 2033.4(10), 8 | 2614.6(3), 8 | 1264.0(2), 4 |
| Density (calcd.), g/cm$^3$ | 1.545 | 1.427 | 1.439 | 1.457 | 1.465 | 1.475 | 2.092 |
| Abs coeff. $\mu$(Mo-K$_\alpha$), mm$^{-1}$ | 0.111 | 0.102 | 0.100 | 0.101 | 0.102 | 0.102 | 6.419 |
| $F$(000) | 500 | 504 | 472 | 928 | 928 | 1200 | 768 |
| Crystal size, mm$^3$ | $0.38 \times 0.12 \times 0.04$ | $0.24 \times 0.22 \times 0.18$ | $0.47 \times 0.24 \times 0.04$ | $0.50 \times 0.05 \times 0.02$ | $1.15 \times 0.22 \times 0.16$ | $0.49 \times 0.16 \times 0.11$ | $0.21 \times 0.17 \times 0.04$ |
| Temperature, K | 100(2) | 100(2) | 100(2) | 100(2) | 146(2) | 173(2) | 173(2) |
| Diffractometer | Stoe-IPDS-II | Stoe-IPDS-II | Stoe-IPDS-II | Stoe-IPDS-II | Siemens-SMART-CCD | Stoe-IPDS-II | Stoe-IPDS-II |
| $\theta$-Range, deg | 2.35 – 27.56 | 2.80 – 27.19 | 2.11 – 25.03 | 2.42 – 25.03 | 1.80 – 32.35 | 1.80 – 26.95 | 3.56 – 25.34 |
| Index ranges | $-28 \le h \le 22$ | $-10 \le h \le 9$ | $-11 \le h \le 11$ | $-19 \le h \le 19$ | $-22 \le h \le 24$ | $-15 \le h \le 15$ | $-9 \le h \le 9$ |
| | $0 \le k \le 4$ | $-22 \le k \le 22$ | $-12 \le k \le 12$ | $-15 \le k \le 15$ | $-7 \le k \le 7$ | $-34 \le k \le 36$ | $-10 \le k \le 10$ |
| | $0 \le l \le 20$ | $-11 \le l \le 11$ | $-13 \le l \le 13$ | $-13 \le l \le 13$ | $-33 \le l \le 33$ | $-9 \le l \le 9$ | $-23 \le l \le 23$ |
| No. of reflections collected | 15908 | 18192 | 10129 | 5933 | 25445 | 31668 | 12493 |
| No. of independent reflections | 1179 | 2498 | 3659 | 1796 | 6454 | 2808 | 1143 |
| $R$(int) | 0.0908 | 0.0495 | 0.0672 | 0.1245 | 0.0808 | 0.0657 | 0.0800 |
| Absorption correction | none | empirical | empirical | empirical | empirical | empirical | Semi-empirical from equivalents |
| $T_{min}$, $T_{max}$ | 0.9591, 09956 | 0.9759, 0.9819 | 0.9547, 0.9960 | 0.9511, 0.9980 | 0.949, 1.000 | 0.9517, 0.9889 | 0.3458, 0.7833 |
| Data/restraints/parameter | 1179/0/84 | 2498/0/172 | 3659/0/311 | 1796/0/154 | 6454/1/308 | 2808/0/200 | 1143/0/93 |
| Goodness of fit on $F^2$ | 0.898 | 1.012 | 1.071 | 1.066 | 1.046 | 1.049 | 1.068 |
| Final $R$ indices [$I > 2\sigma(I)$], $R1$, $wR2$ | 0.0678, 0.1669 | 0.0366, 0.0807 | 0.1174, 0.3316 | 0.1071, 0.2604 | 0.0625, 0.0794 | 0.0369, 0.0962 | 0.0477, 0.1173 |
| $R$ indices (all data) | 0.1224, 0.1808 | 0.0531, 0.0857 | 0.1523, 0.3512 | 0.1796, 0.3256 | 0.0955, 0.1498 | 0.0399, 0.0987 | 0.0594, 0.1315 |
| Largest diff. peak/hole eÅ$^{-3}$ | 0.362/−0.301 | 0.251/−0.23 | 1.148/−0.488 | 0.476/−0.508 | 0.244/−0.225 | 0.260/−0.188 | 1.118/−1.091 |

* The molecule contains no anomalous scattering atoms. Thus the absolute structure of the polar crystal could not be established.

Table 4. Relative amounts of **1** – **4** in reaction mixtures **A**, **B** and **C**.

| | **1** | **2** | **3** | **4** |
|---|---|---|---|---|
| Retention time [min] | 2.73 | 13.04 | 11.03 | 18.0 |
| Concentration in sample reaction A [mmol/l] | 1.78 | 1.27 | 0.76 | 0.59 |
| Concentration in sample reaction B [mmol/l] | 1.47 | 0.53 | 0.45 | 0.7 |
| Concentration in sample reaction C [mmol/l] | 1.47 | 1.25 | 1.08 | 0.61 |

compound **3ox** (0.170 g, 0.71 mmol, 71%) as orange blocks. $^1$H NMR (250 MHz, $CDCl_3$): $\delta = 6.51$ (dd, $J = 1.5$ Hz, 2 H), 7.38 (s, 2 H), 7.78 (d, $J = 1.5$ Hz, 2 H), 8.63 (dd, $J = 2.5$ Hz, 2 H). IR (KBr): $\upsilon_{max} = 1663$, 1661, 1659, 1603, 1589 cm$^{-1}$. MS (ESI): $m/z = 240$ [M$^+$]. $C_{12}H_8N_4O_2$ (240.22): calcd. C 60.00, H 3.36, N 23.32; found C 59.76, H 3.24, N 22.92.

*Preparation of* **3qh**: A solution of **3** (2.66 g, 11 mmol) in 100 ml of ethanol was stirred for two days in air. Black **3qh** was precipitated. After filtering the residue was washed with 20 ml of dichloromethane. X-ray powder diffraction of this insoluble material shows exclusively the pattern of **3qh** (2.27 g, 9.42 mmol, 86%). IR (KBr): $\upsilon_{max} = 1654$, 1600, 1591, 1536, 1524 cm$^{-1}$. $C_{12}H_9N_4O_2$ (241.23): calcd. C 59.75, H 3.76, N 23.23; found C 59.84, H 3.86, N 22.92.

Upon storing **3** for two weeks in air, black single crystals of **3qh** suitable for X-ray diffraction were obtained from a 0.1 M solution of **3** in methanol.

### *Syntheses of salts with the semiquinone radical anions **2sq**$^-$ and **3sq**$^-$*

*Formation of* **2sq**$^-$: **2** (0.002 g, 0.01 mmol) and potassium *tert*-butoxide (0.011 g, 0.10 mmol) were dissolved in 1 ml of isopropanol in an atmosphere of argon. The pale yellow solution formed was transferred *via* syringe into a Schlenk EPR tube and cooled to −78 °C.

*Formation of* **3sq**$^-$: **3** (0.003 mg, 0.01 mmol) and potassium *tert*-butoxide (0.011 g, 0.10 mmol) were dissolved in 1 ml isopropanol in an atmosphere of argon. The pale yellow solution formed was transferred *via* syringe into a Schlenk EPR tube and cooled to −78 °C.

### *Syntheses of the hydroquinones **5** and **7***

*Preparation of* **5**: Pyrazole (1.23 g, 18 mmol) and 1,4-naphthoquinone (2.85 g, 18 mmol) in 300 ml of ethanol were heated under reflux for 16 h. The hot solution was filtered. Addition of water to the filtrate resulted in the precipitation of 2-(pyrazol-1-yl)-1,4-dihydroxynaphthalene. Recrystallisation (dichloromethane) of this material afforded compound **5** (1.40 g, 6.2 mmol, 34.4%) as white needles. $^1$H NMR (250 MHz, $CDCl_3$): $\delta = 6.51$ (dd, $J = 2.25$ Hz, 1 H), 6.94 (s, 1 H), 7.54 (m, 2 H), 7.76 (d, $J = 2.25$ Hz, 1 H), 7.95 (d, $J = 2.5$ Hz, 1 H), 8.20 (m, 2 H). MS (ESI): $m/z = 226$ [M]$^+$. $C_{13}H_{10}N_2O_2$ (226.23): calcd. C 69.02, H 4.46, N 12.38; found C 68.85, H 4.32, N 12.12.

*Preparation of* **7**: 1,4-Benzoquinone (8.76 g, 81.04 mmol) and 4-bromopyrazole (11.99 g, 81.58 mmol) were suspended in 200 ml of carefully degassed ethanol. The mixture was heated to reflux for 18 h, whereupon a brown solution formed. When the solution was cooled to r. t., a brown precipitate formed. The solid material was filtered off and recrystallized from hot ethanol. Yield: 2.27 g (5.67 mmol, 14%). $^1$H NMR (250 MHz, d$^6$-DMSO): $\delta = 10.33$ (s, 2 H), 8.62 (s, 2 H), 7.96 (s, 2 H), 7.52 (s, 2 H). $^{13}$C NMR (62.9 MHz, d$^6$-DMSO): $\delta = 141.0$, 140.1, 131.4, 125.8, 111.4, 93.3. MS (ESI): $m/z = 400$ [M]$^+$. $C_{12}H_8Br_2N_4O_2$ (400.05): calcd. C 36.03, H 2.02, N 14.01; found C 35.98, H 2.04, N 13.78.

### *Syntheses of the quinones **5ox**, **6ox**, and **7ox***

*Preparation of* **5ox**: **5** (1.06 g, 4.71 mmol) and 1,4-benzoquinone (0.51 g, 4.71 mmol) were dissolved in 100 ml of ethanol and stirred at r. t. for five hours under an atmosphere of nitrogen. After cooling the reaction mixture to 0 °C, 2-(pyrazol-1-yl)-1,4-dihydroxynaphthalene precipitated. Recrystallisation (*n*-propanol) of this material afforded compound **5ox** (0.39 g, 1.74 mmol, 37.0%) as yellow needles. (Found: **5ox**$^+$ 225, requires: % **5ox**$^+$ 224). $^1$H NMR (250 MHz, $CDCl_3$): $\delta = 6.17$ (dd, $J = 2.0$ Hz, 1 H), 7.24 (s, 1 H), 7.40 (m, 2 H), 7.42 (d, $J = 2.75$ Hz, 1 H), 7.80 (m, 2 H), 8.34 (d, $J = 2.75$ Hz, 1 H). MS (ESI): $m/z = 225$ [M+H]$^+$. $C_{13}H_8N_2O_2$ (224.21): calcd. C 69.64, H 3.60, N 12.49; found C 69.73, H 3.49, N 12.25.

The orthorhombic polymorph was obtained by recrystallisation from dichloromethane.

*Preparation of* **6ox**: Pyrazole (23.49 g, 345 mmol) and 2,3-dichloro-1,4-naphthoquinone (13.05 g, 57.5 mmol) in 200 ml of ethanol were heated under reflux for 24 h. After cooling the reaction mixture to 0 °C, 2,3-bis(pyrazol-1-yl)-1,4-naphthoquinone precipitated. Recrystallisation of this material from ethanol afforded compound **6ox** (5.12 g, 6.2 mmol, 17.70 mmol, 30.8%) as thin orange needles. $^1$H NMR (250 MHz, $CDCl_3$): $\delta = 6.43$ (dd, $J = 1.8$ Hz, $J = 2.5$ Hz, 2 H), 7.54 (dd, $J = 1.8$ Hz, 2 H), 7.80 (dd, $J = 0.5$ Hz, $J = 2.5$ Hz, 2 H), 7.85 (dd, $J = 3.5$ Hz, $J = 5.0$ Hz, 2 H), 8.23 (dd, $J = 3.5$ Hz, $J = 5.0$ Hz, 2 H). MS (ESI): $m/z = 290$ [M]$^+$. $C_{16}H_{10}N_4O_2$ (290.28): calcd. C 66.20, H 3.47, N 19.30; found C 66.07, H 3.35, N 19.04.

*Preparation of* **7ox**: A solution of DDQ (0.23 g, 1 mmol) in 20 ml of dioxane was added dropwise to a stirred solution of **7** (0.41 g, 1 mmol) in 200 ml of dioxane at r. t. After the mixture had been stirred for one hour, the orange mother liquor was filtered off the white precipitate. The mother liquor was taken to dryness *in vacuo*, redissolved in a minimum amount of dichloromethane, filtered and taken to dryness again. Recrystallisation ($CH_2Cl_2$) of this material afforded compound **7ox** (0.18 mg, 0.45 mmol, 45%) as orange crystals.

$^1$H NMR (250 MHz, d$^6$-DMSO): $\delta = 8.51$ (s, 2 H), 7.86 (s, 2 H), 7.40 (s, 2 H). MS (ESI): $m/z = 398$ $[M]^+$. $C_{12}H_6Br_2N_4O_2$ (398.01): calcd. C 36.21, H 1.52, N 14.08; found C 36.23, H 1.66, N 14.08.

*Electrochemistry*

Anhydrous 99.9%, HPLC grade dichloromethane for electrochemistry was purchased from Aldrich Chemicals. The supporting electrolyte used was electrochemical grade $NBu_4PF_6$ obtained from Fluka. Cyclovoltammetry was performed in a three-electrode cell with a platinum working electrode surrounded by a platinum spiral counterelectrode and the aqueous saturated calomel reference electrode (SCE) mounted with a Luggin capillary. Either a BAS 100A or a BAS 100W electrochemical analyzer was used as a polarizing unit.

*X-ray crystallography*

Data collection: STOE IPDS II two-circle diffractometer [**2**, **3qh**, **4**, **5**, **5ox(monoclinic)**, **6ox**, **7ox**], Siemens-SMART-CCD three-circle diffractometer [**5ox(orthorhombic)**], graphite monochromated Mo-K$_\alpha$ radiation ($\lambda = 0.71703$ Å), T = 173(2) K. Empirical absorption corrections were performed using SADABS [22] [**5ox(orthorhombic)**] or the MULABS [23] option [**2**, **3qh**, **4**, **5**, **5ox(monoclinic)**, **6ox**, **7ox**] in PLATON [24]. The structures were solved by direct methods using the program SHELXS [25] and refined against $F^2$ with full-matrix least-squares techniques using the program SHELXL-97 [26]. All non-hydrogen atoms were refined with anisotropic displacement parameters. Hydrogen atoms were located by difference Fourier synthesis and refined using a riding model. Crystallographic data (excluding structure factors) for the structures reported in this paper have been deposited with the Cambridge Crystallographic Data Centre as supplementary publication nos. CCDC 202035 [**2**], CCDC 202039 [**3qh**], CCDC 202037 [**4**], CCDC 202038 [**5**], CCDC 202040 [**5ox(monoclinic)**], CCDC 202034 [**5ox(orthorhombic)**], CCDC 202036 [**6ox**] and CCDC 281847 [**7ox**]. Copies of the data can be obtained free of charge on application to CCDC, 12 Union Road, Cambridge CB2 1EZ (Telefax: +1223/336 033; E-mail: deposit@ccdc.cam.ac.uk).

*Acknowledgements*

M.W. is grateful to the "Deutsche Forschungsgemeinschaft" (DFG) for financial support. G.M. wishes to thank the "Fonds der Chemischen Industrie" (FCI) and the "Bundesministerium für Bildung und Forschung" (BMBF) for a Ph. D. grant. P.Z. gratefully acknowledges the financial support of the University of Siena.

[1] A. M. Allgeier, C. A. Mirkin, Angew. Chem. Int. Ed. **37**, 894 (1998).
[2] T. Hirao, Coord. Chem. Rev. **226**, 81 (2002).
[3] M. Mure, Acc. Chem. Res. **37**, 131 (2004).
[4] J. Catalan, F. Fabero, M. S. Guijarro, R. M. Claramunt, M. D. S. Maria, M. d. l. C. Foces-Foces, F. H. Cano, J. Elguero, R. Sastre, J. Am. Chem. Soc. **112**, 747 (1990).
[5] P. Cornago, C. Escolástico, M. D. S. María, R. M. Claramunt, D. Carmona, M. Esteban, L. A. Oro, C. Foces-Foces, A. L. Llamas-Saiz, J. Elguero, J. Organomet. Chem. **467**, 293 (1994).
[6] T. E. Keyes, P. M. Jayaweera, J. J. McGarvey, J. G. Vos, J. Chem. Soc., Dalton Trans. 1627 (1997).
[7] T. E. Keyes, R. J. Forster, P. M. Jayaweera, C. G. Coates, J. J. McGarvey, J. G. Vos, Inorg. Chem. **37**, 5925 (1998).
[8] R. Dinnebier, H.-W. Lerner, L. Ding, K. Shankland, W. I. F. David, P. W. Stephens, M. Wagner, Z. Anorg. Allg. Chem. **628**, 310 (2002).
[9] B. Wolf, S. Zherlitsyn, B. Lüthi, N. Harrison, U. Löw, V. Pashchenko, M. Lang, G. Margraf, H.-W. Lerner, E. Dahlmann, F. Ritter, W. Assmus, M. Wagner, Phys. Rev. **69B**, 092403 (2004).
[10] A. V. Prokofiev, E. Dahlmann, F. Ritter, W. Assmus, G. Margraf, M. Wagner, Cryst. Res. Technol. **39**, 1014 (2004).
[11] A. V. Prokofiev, E. Dahlmann, F. Ritter, W. Assmus, G. Margraf, M. Wagner, J. Crystal Growth **275**, e2025 (2005).
[12] B. Wolf, A. Brühl, J. Magerkurth, S. Zherlitsyn, V. Pashchenko, B. Brendel, G. Margraf, H.-W. Lerner, M. Wagner, B. Lüthi, M. Lang, J. Magn. Magn. Mater. **290 – 291**, 411 (2005).
[13] G. Margraf, T. Kretz, F. F. d. Biani, F. Laschi, S. Losi, P. Zanello, J. W. Bats, B. Wolf, K. Remović-Langer, M. Lang, A. Prokofiev, W. Assmus, H.-W. Lerner, M. Wagner, Inorg. Chem. **45**, 1277 (2006).
[14] G. Margraf, J. W. Bats, M. Bolte, H.-W. Lerner, M. Wagner, Chem. Commun. 956 (2003).
[15] W. Gauß, H. Heitzer, S. Petersen, Liebigs Ann. Chem. **764**, 131 (1972).
[16] P. Ballesteros, R. M. Claramunt, C. Escolastico, M. D. S. Maria, J. Elguero, J. Org. Chem. **57**, 1873 (1992).
[17] M. Kubinyi, G. Keresztury, Spectrochim. Acta, Part A **45**, 421 (1989).
[18] L. Ding, F. F. d. Biani, M. Bolte, P. Zanello, M. Wagner, Organometallics **19**, 5763 (2000).
[19] M. Bolte, H.-W. Lerner, Private Communication, CCDC 160100 (2001).
[20] Crystallographic data of **2** (CCDC 202035): $C_9H_8N_3O_2$, T = 173(2) K, Mo-K$_\alpha$, $\lambda = 0.71073$ Å, no. of reflections 27809, no. of independent reflec-

tions 1086. $R1 = 0.0391$, $wR2 = 0.0848[I > 2\sigma(I)]$. Crystal system: orthorhombic, $P2_12_12_1$, $Z = 4$, $a = 4.6642(5)$ Å, $b = 11.0730(10)$ Å, $c = 15.3260(10)$ Å, $V = 791.54(12)$ Å$^3$; see also ref. [4].

[21] T. Sakurai, Acta Crystallogr. **B24**, 403 (1968).

[22] G. M. Sheldrick, SADABS, University of Göttingen, Germany (2000).

[23] R. H. Blessing, Acta Crystallogr. Sect. A **51**, 33 (1995).

[24] A. L. Spek, Acta Crystallogr. Sect. A **46**, C34 (1990).

[25] G. M. Sheldrick, Acta Crystallogr. Sect. A **46**, 467 (1990).

[26] G. M. Sheldrick, SHELXL-97, A Program for the Refinement of Crystal Structures, University of Göttingen, Germany (1997).